



ORIGINAL RESEARCH

Two-stage self-adaption security and low-carbon dispatch strategy of energy storage systems in distribution networks with high proportion of photovoltaics

Lei Chen¹  | Wei Tang¹ | Lu Zhang¹  | Zhaoqi Wang¹  | Jun Liang²

¹College of Information and Electrical Engineering, China Agricultural University, Beijing, China

²School of Engineering, Cardiff University, Cardiff, UK

Correspondence

Wei Tang.
Email: wei_tang@cau.edu.cn

Funding information

Research and Development of Key Technologies for Economic and Low-Carbon Regulation of New-Type Rural Power Grids with Massive Distributed Resources, Grant/Award Number: 1400-202155508A-0-5-ZN

Abstract

With the goal of achieving carbon neutrality, active distribution networks (DNs) with a high proportion of photovoltaics (PVs) are facing challenges in maintaining voltage stability and low-carbon operation. Energy storage systems (ESSs), which have the ability to store and transfer energy temporarily, can be used as effective measures to enhance the capacity of consuming PVs and reduce carbon emissions in DN. However, existing low-carbon dispatch strategies for multiple sources, storages and loads fail to consider voltage violations, while the temporal carbon emission intensity of the upper-level power grid is also often overlooked, which is an important factor that affects the dispatch strategy. Therefore, a two-stage self-adaptive dispatch strategy of ESSs that considers the temporal characteristics of slack nodal carbon emission intensity to minimise carbon emissions while maintaining voltage stability in DN with high access to PVs is proposed. First, the framework of the proposed two-stage self-adaptive dispatch strategy of ESSs is established by taking into account the effects of ESSs on adjusting voltages and reducing carbon emissions, respectively, with the two-stage switch principle of two operation modes being determined. On this basis, an optimization dispatch model is established to improve voltages and carbon emissions, and the optimal day-ahead dispatch strategy of ESSs can be obtained by solving the model using genetic algorithm. Case studies of the modified 10 kV IEEE 33-node DN and IEEE 123-node DN verify the feasibility and superiority of the proposed two-stage self-adaptive security and low-carbon day-ahead dispatch strategy for ESSs, showing that the voltage stabilisation and lower carbon emissions of DN are both improved.

KEYWORDS

distribution network, energy storage, genetic algorithm, photovoltaic power systems

1 | INTRODUCTION

In the process of achieving the goal of carbon peaking and carbon neutrality [1, 2], clean energies represented by distributed photovoltaics (proportion of photovoltaics (PVs)) have developed rapidly due to the advantages of carbon emission reduction and environmental protection. As important measures to achieve carbon neutrality, high proportion renewable energies gradually come into being the initial components of active distribution networks (DNs) [3].

Due to the wide coverage and poor structural strength of DN, large-scale distributed PVs will lead to a series of problems, such as voltage violation and insufficient capacity of feeders [4, 5], which greatly affect the secure and economic operation of DN. Moreover, due to loads are dispersed in DN whose power supply radiuses are always large. Considering the strong intermittence and randomness, the distributed PVs are difficult to be consumed locally. Therefore, to improve the carbon emission reduction effect of DN promoting PV consumption, the storage and temporal transfer of low-carbon

This is an open access article under the terms of the [Creative Commons Attribution-NonCommercial-NoDerivs](https://creativecommons.org/licenses/by-nc-nd/4.0/) License, which permits use and distribution in any medium, provided the original work is properly cited, the use is non-commercial and no modifications or adaptations are made.

© 2023 The Authors. *IET Smart Grid* published by John Wiley & Sons Ltd on behalf of The Institution of Engineering and Technology.

electricity can be realized by distributed energy storage systems (ESSs).

The existing researches to achieve high proportion of PV consumption in DNs utilising distributed ESSs mainly aim at shedding peak loads and filling valley loads [6], reducing operation costs [7] and reducing voltage deviation [8, 9]. In ref. [10], a local control model of ESS charging/discharging was constructed. By inputting the node voltage deviation and the state of charge of the ESSs in the fuzzy neural network, the local control was realized. On this basis, considering the communication ability of DNs, a multi-stage control including distributed-local and centralised-local modes of ESSs was proposed in ref. [11, 12]. Under the centralised control architecture, based on the scenario clustering method, the authors in ref. [7] constructed a long-term scale ESS planning and operation integrated optimization model, which realized the joint reduction of power purchase costs, power losses and power fluctuations on the tie line. In ref. [13], based on generalised ESSs, an active energy management model of microgrids using potential games was constructed to promote the consumption of uncertain renewable energies based on the conditional value at risk. In ref. [14], the constraints of carbon footprint and tie line power deviation were further considered, and the operation with multiple temporal scales was realized based on ESSs, on this basis the optimal allocation of ESSs was realized in active DNs.

However, the existing researches on PV consumption in DNs using distributed ESSs mainly aim at voltage regulation, peak load regulation, and power loss reduction. For the purpose of power loss reduction, the balance between PVs' output powers and power demand of loads should be realized in local through the dispatch of ESSs, so as to reduce the risk of undervoltage and overvoltage while reducing the power loss. When PVs' output powers increase to a certain extent, the PVs' output powers are higher than power demand of loads and the residual power will be injected into DNs, which will cause the increase of power in DNs, and then increase the power loss and raise the voltage. For the purpose of carbon emission reduction, the carbon emission intensity of the upper-level power grid is greater than that of the PVs. Under the premise of ensuring that voltages do not exceed the limit, the low-carbon power generated by PVs should be absorbed as much as possible through the dispatch of ESSs. Therefore, the existing researches are difficult to fully utilise clean energy and hard to maximise the carbon emission reduction with the constraints of the secure and stable operation of DNs.

The existing researches on realizing low-carbon operation control of DNs by using distributed ESSs are aiming at making full use of low-carbon clean energy through orderly charging/discharging of ESSs. In hybrid microgrids containing wind turbines, PVs and ESSs, the authors in ref. [15] reduced the carbon emissions in smart microgrids and improved the power supply reliability of microgrids by optimising the installed capacity ratio of wind turbines, PVs and ESSs. In addition, the authors in ref. [16, 17] proved the advantages of ESSs in matching clean energy output power and power demand of loads. By fully using clean energy such as PVs, wind turbines and hydro powers, a significant reduction of carbon

emissions can be achieved on the condition of source-load matching. In ref. [18], considering the rising demand of electric vehicles, a collaborative optimization model of rooftop PVs and ESSs providing electricity for electric vehicles was proposed, which is an effective measure to realize the net-zero carbon emission of electrified transportation. On this basis, the authors in ref. [19] considered the uncertainty of sources and loads of DNs, and used the information gap decision theory to construct the optimization planning model of the mobile ESSs, and the coordinated operation of distributed PVs, DNs, loads and ESSs was realized to reduce carbon emissions. On the basis of improving the carbon emission reduction ability of DNs, the comprehensive cost of the whole DN was cut simultaneously.

However, the existing low-carbon dispatch methods of ESSs in DNs are proposed on the basis of a constant carbon emission intensity of the upper-level power grid. Since the carbon emissions of DNs are mainly related to the upper-level power grid, which is composed of power sources with different carbon emission intensities, such as gas turbines, PVs and wind turbines. The output powers of PVs, wind turbines and other units have the temporal fluctuation characteristics, it can be known that the carbon emission intensity of the upper-level power grid also has temporal fluctuation characteristics according to the principle of proportional sharing [20]. The existing researches still lack the consideration of the temporal characteristics of the carbon emission intensity of the upper-level power grid, which makes it difficult for the low-carbon operation strategy of PVs and ESSs to cope with the frequent fluctuations of the carbon emission intensity of the upper-level power grid.

Besides, there are lots of mathematical programming methods to solve the existing optimization models in planning and dispatching of power systems. Recently, convex relaxation methods, such as the second-order cone relaxation [21] and the semi-definite relaxation [22], have been implemented to solve optimal power flow (OPF) owing to their computational benefits. It is confirmed in [23] that although second-order cone programming is an efficient instrument for convexifying AC OPF equations, it is unable to reach the global optimal solution compared to other methods. In ref. [24], a tri-level model of the energy management problem of the power DNs was proposed, and then a quadruple-loop solution procedure was developed for the proposed tri-level energy management model, including two column-and-constraint (C&CG) loops for the two-stage decision-making framework, and two sequential mixed integer second-order cone programme loops to enhance the solution feasibility with respect to the non-convex power flow and Weymouth equations.

However, there are still shortcomings of mathematical programming methods lying in solving nonlinear programming with absolute value functions, and these methods also fail to deal with multi-stage switches of operation modes. As a consequence, heuristic algorithms are widely utilised for the capabilities of demodelling and global optimization.

In order to solve the above shortcomings, this paper proposes a day-ahead security and low-carbon optimal dispatch

method of ESSs in DNs with high proportion PVs. Firstly, considering the advantages of ESSs in consuming high-proportion distributed PVs and reducing carbon emissions in DNs, a self-adaption day-ahead optimal dispatch framework of ESSs is proposed to control voltage and reduce carbon emissions, and then the switch principle of two operation modes is formulated. Then, the voltage regulation model of ESSs is constructed with the objective of the minimum voltage deviation of all nodes in the DN, and the carbon emission reduction model is constructed with the objective of minimum carbon emissions of the DN. Finally, considering the demodelling characteristics of heuristic algorithms in solving nonlinear programming, the genetic algorithm (GA) is used to solve the dual-mode collaborative optimization operation dispatch of ESSs in the security and low-carbon DN. The feasibility and superiority of the proposed two-stage self-adaption security and low-carbon dispatch strategy of ESSs in DNs with high proportion PVs are verified by a modified 10 kV IEEE 33-node DN and IEEE 123-node DN.

The main contribution of the proposed dual-mode dispatch strategy of ESSs is to enhance the security and decarbonisation of DNs, and then contribute to the construction of low-carbon energy systems. The main reason is that the carbon reducing capability of multiple resources and loads can be fully utilised, and then the flexible interaction of sources and loads can be realized to improve the decarbonisation jointly. On the basis of the proposed self-adaption switch principle, the automation and intelligence of DNs can be fully taken advantage of in the centralised control of energy systems.

2 | FRAMEWORK OF TWO-STAGE SELF-ADAPTION SECURITY AND LOW-CARBON DISPATCH STRATEGY OF ESS

2.1 | Two-stage dispatch strategy of ESSs in distribution networks via dual operation modes switching

Since the temporal output power of PVs and power demand of loads serve different tendencies, the high proportion of PVs accessing to DNs will cause the excessive voltage violation risk, and the clean energy consumption capacity of the DN is insufficient. Due to the capability of ESSs to transfer electricity temporally, it is necessary to dispatch ESSs orderly to control the risk of voltage violation. On the one hand, considering the effects of high proportion PVs on the security operation in DNs, this paper proposes a dual-mode optimization dispatch strategy of ESSs. On the other hand, the carbon emission reduction model is further constructed to realize the low-carbon operation of DNs. And based on the above two modes, the self-adaption dispatch strategy for ESSs is proposed to improve the security and reduce the carbon emission of DNs, which can contribute to the goal of carbon neutralisation.

The switch principle for two dispatch modes are as follows:

$$\Omega(t) = \begin{cases} 1 & \Omega(t-1) = 1 & \& \forall U_i^*(t) \notin [0.94U_0^*, 1.06U_0^*] \\ 2 & \Omega(t-1) = 1 & \& \forall U_i^*(t) \in [0.94U_0^*, 1.06U_0^*] \\ 1 & \Omega(t-1) = 2 & \& \forall U_i^*(t) \notin [0.93U_0^*, 1.07U_0^*] \\ 2 & \Omega(t-1) = 2 & \& \forall U_i^*(t) \in [0.93U_0^*, 1.07U_0^*] \end{cases} \quad (1)$$

where $\Omega(t)$ is the dispatch mode of ESSs at moment t ; $U_i^*(t)$ is the per unit voltage of node i at moment t , $i \in [1, N]$, N is the number of nodes and U_0^* is the per unit value of the rated voltage.

As shown in Figure 1, the dispatch strategy proposed in this paper includes 2 modes: one is the voltage regulation mode, the other is the low-carbon operation mode. The charging/discharging dispatch mode of ESSs can be determined by assessing the voltage deviation of nodes in each dispatch period. The specific dispatch modes are as follows:

- (1) Mode 1: Voltage regulation mode. Once voltage violation exists in the DN, the distributed ESSs switch to Mode 1 aiming at reducing the node voltage deviation by fully using the active power regulation ability of ESSs, and the secure and stable operation of the DN are maintained. It should be noted that in the voltage regulation mode, the impact of high proportion of PVs access to DNs on node voltage needs to be fully considered. In this operation mode, if the voltage violation in the next dispatch period is avoided and out of the dead zone range of ± 0.01 p. u., the operation mode will be quickly switched to Mode 2.
- (2) Mode 2: Low-carbon operation mode. When the node voltages of the whole DN are maintained within the range of $[0.93 U_0^*, 1.07 U_0^*]$, the distributed ESSs operate in the low-carbon dispatch mode aiming at making full use of the temporal transfer capability of consuming PVs to reduce the carbon emissions of the DN. It should be noted that in the low-carbon dispatch mode, the temporal characteristics of the carbon emission intensity of the upper-level power

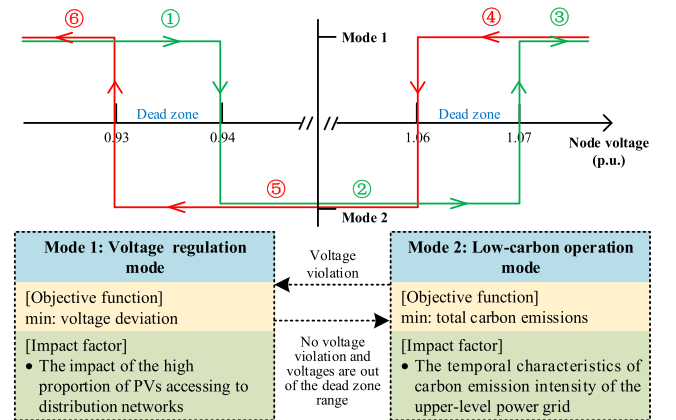


FIGURE 1 Framework of self-adaption security and low-carbon day-ahead dispatch strategy of energy storage systems.

grid needs to be fully considered. In this operation mode, if a voltage violation occurs in the next dispatch period, the operation will be quickly switched back to Mode 1.

In Figure 1, the green line shows the change state of increasing voltage. When the voltage is less than 0.93 p. u., the DN operates under Mode 1 as shown in zone ①. As the voltage rises to 0.94 p. u., the operation mode will be switched to Mode 2, note that the dead zone is crossed. Then, the operation mode switches to Mode 1 again when the voltage rises to 1.07 p. u. The red line shows the change state of decreasing voltage. When the voltage is more than 1.07 p. u., the DN operates under Mode 1 as shown in zone ④. As the voltage decreases to 1.06 p. u., the operation mode will be switched to Mode 2, note that the dead zone is crossed. Then, the operation mode switches to Mode 1 again when the voltage decreases to 0.93 p. u.

In addition, for the power supply capacity and quality problems of the DN, such as new energy consumption and voltage regulation, there are also effective means such as reactive power regulation of photovoltaic inverters, which can provide voltage support capacity for the DN under safe operation mode. The self-adaption security and low-carbon day-ahead dispatch architecture proposed in this paper is also universal.

On the basis of the proposed single optimization model in Stage I, we further execute Stage II to fully ensure the voltage safety in both voltage regulation mode and low-carbon operation mode. So a two-stage dual-mode dispatch strategy of ESSs is established. The process of switching between the safe low-carbon dual-mode operation is divided into two stages. The goal is to prevent voltage safety issues in the low-carbon operation mode, ensuring the safe operation of the DN in any operational scenario, and maximising carbon reduction capabilities based on this foundation.

In Stage I, ESSs operation mode of the current dispatch period is preliminarily determined based on the ESSs operation mode of the previous dispatch period and the voltage range of all nodes at the beginning of the current dispatch period, according to Formula (1). Specifically, if the voltage of any node is less than 0.94 p.u. or greater than 1.06 p.u., and the operation mode of the previous dispatch period was Mode 1, then the operation mode of the current dispatch period will be Mode 1. If the voltage of any node is less than 0.93 p.u. or greater than 1.07 p.u., and the operation mode of the previous dispatch period was Mode 2, then the operation mode of the current dispatch period will be switched to Mode 1. When the voltage of any node is in the range of 0.94 p.u.–1.06 p.u., and the operation mode of the previous dispatch period was Mode 1, the operation mode of the current dispatch period is preliminarily determined to be Mode 2. When the voltage of any node is in the range of 0.93 p.u.–1.07 p.u., and the operation mode of the previous dispatch period was Mode 2, the operation mode of the current dispatch period is preliminarily determined to be Mode 2.

In Stage II, if ESSs operation mode of the current dispatch period is determined to be Mode 1 in Stage I, it will be the final ESSs operation mode. If ESSs operation mode of the current dispatch period is determined to be Mode 2 in Stage I, the

optimal charging/discharging strategy of ESSs need to be calculated under Mode 2, and the voltage of all nodes need to be obtained by power flow calculation. Then, the voltage is verified again according to Formula (1) to finally determine ESSs operation mode of the current dispatch period. The flowchart of two-stage dispatch strategy of ESSs in DN via multiple operation modes switching is shown in Figure 2.

2.2 | Spatiotemporal carbon emission flow calculation based on power flow of distribution network

Based on power flow calculation of the DN, the active power of each node and branch can be obtained. Combined with the principle of proportional sharing [20], the carbon emission flow intensity of each node and carbon emission flow intensity of each branch can be accurately calculated, thereby accurately depicting the spatiotemporal distribution characteristics of the carbon flow of the DN. Based on the known temporal carbon emission intensity of the upper-level power grid $e_G(t)$, the nodal carbon intensity of each node e_j can be calculated. Furthermore, since the carbon emission flow intensity of each branch ρ_{ij} is equal to the nodal carbon intensity of the head node of that branch e_i , the nodal carbon intensity of each node can be expressed as:

$$e_j(t) = \begin{cases} e_G(t) & j = 0 \\ \sum_{j \in \delta} \frac{P_{ij}(t)\rho_{ij}(t) + P_j^{\text{DG}}(t)e_j^{\text{DG}}(t)}{P_{ij}(t) + P_j^{\text{DG}}(t)} & j \in [1, n-1] \end{cases} \quad (2)$$

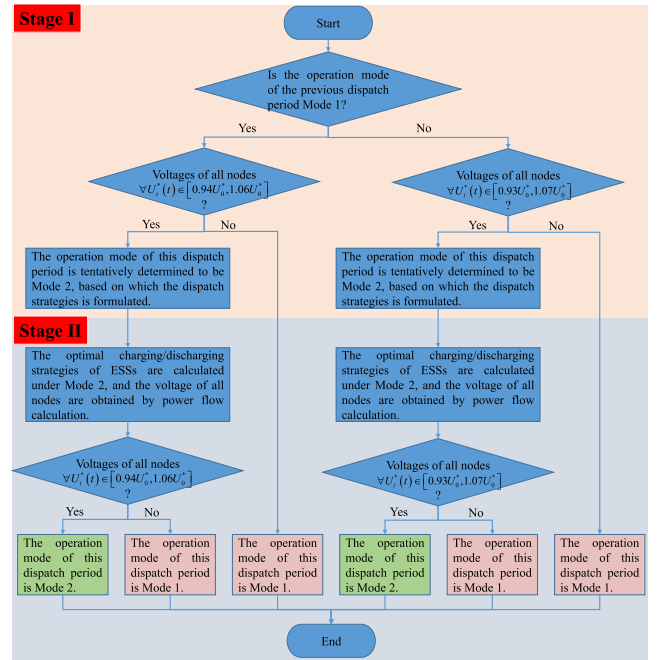


FIGURE 2 The flowchart of two-stage dispatch strategy of energy storage systems in distribution networks via multiple operation modes switching.

where i and j are the first and last nodes of the branch respectively; n is the total number of nodes in the DN; δ is the set of all nodes; P_{ij} is the active power of the branch, and P_j^{DG} is the active power of the DG at node j ; e_j^{DG} is the carbon emission intensity of the DG at node j ; note that the carbon emission intensity of the PV is 0 kgCO₂/kWh.

In the low-carbon operation mode, the charging/discharging state of the ESS depends on the relationship between its internal carbon intensity and the nodal carbon intensity of the node that the ESS has access to. Therefore, the charging/discharging principles of ESSs aimed at reducing carbon emissions are as follows:

- 1) When the nodal carbon intensity of the node that the ESS has accessed to is higher than the internal carbon intensity of the ESS at the current time, and the remaining electricity in the ESS is not less than the lower limit value allowed, the ESS works in a discharging state.
- 2) When the nodal carbon intensity of the node that the ESS has accessed to is lower than the internal carbon intensity of the ESS at the current time, and the remaining electricity in the ESS is less than the upper limit value allowed, the ESS works in a charging state.
- 3) When the nodal carbon intensity of the node that the ESS has accessed to is equal to the internal carbon intensity of the ESS at the current time, the ESS does not operate.
- 4) When the remaining electricity in the ESS is zero, the internal carbon intensity of the ESS at the current time cannot be calculated. Therefore, the ESS works in a charging state to ensure that the internal carbon intensity of the ESS exists in the next time period and can be used to determine the operation strategy of the ESS.

3 | DUAL-MODE DAY-AHEAD OPTIMAL DISPATCH MODEL OF ESS

In this paper, the charging/discharging powers of ESSs are taken as the control variables. In Mode 1, the minimum voltage deviation of all nodes in the DN is taken as the optimization objective. In Mode 2, the minimum carbon emission of the whole DN is taken as the optimization objective. Under the premise of satisfying the constraints of node voltage, branch current, output active/reactive power of PVs, power flow and branch power, the low-carbon day-ahead optimization dispatch of ESSs is realized based on the self-adaption switch of operation modes in the DN.

3.1 | Objective function

- (1) Mode 1: Voltage regulation mode

In order to ensure the secure and stable operation of DNs, the optimization model of Mode 1 is constructed with the objectives of minimum voltage deviation of all nodes, per-unit

value of net power and the per-hour dispatch cost of ESSs in the whole DN in the typical day. On this basis, the dispatch cost of ESSs is further considered, the optimization objective can be expressed as

$$\min F_1 = \int_{t \in \Psi_1} \left(\sum_{i=1}^n |U_i^*(t) - U_0^*| / U_0^* + P_{\max}(t) / P_{\text{base}} + \mu_1 C_{\text{ESS}} \right) dt \quad (3)$$

where the set Ψ_1 represents the time period when ESSs operate under Mode 1; $P_{\max}(t)$ is the maximum net power of the whole DN; P_{base} is the reference value of power; μ_1 is the charging/discharging cost coefficient of ESSs under Mode 1; C_{ESS} is the per-hour dispatch cost of ESSs.

$$C_{\text{ESS}} = C_{\text{op}} |P_{\text{ESS}}^t| + \frac{C_{\text{ins}}}{365 \times 24 L_S} \quad (4)$$

where C_{op} is the per-watt operational and maintenance cost; C_{ins} is the per-watt installation cost; L_S is the life cycle of ESSs.

- (2) Mode 2: Low-carbon operation mode

In order to realize the day-ahead low-carbon optimal dispatch of DNs, Mode 2 constructs an optimization model with the objective of the minimum carbon emission and the per-hour dispatch cost of ESSs in the whole DN in a typical day. The optimization objective can be expressed as

$$\min F_2 = \int_{t \in \Psi_2} \left(\sum_{i \in [0, n]} P_{ij}(t) \rho_{ij}(t) + e_j(t) P_j(t) + \mu_2 C_{\text{ESS}} \right) dt \quad (5)$$

where the set Ψ_2 represents the time period when ESSs operate under Mode 2; μ_2 is the charging/discharging cost coefficient of ESSs under Mode 2.

3.2 | Constraint condition

During the day-ahead optimization dispatch of ESSs shown in Mode 1 and Mode 2, the following constraints should be accurately preserved during the optimization process, such as node voltage, branch current, output active/reactive power of PVs, inverter capacity, power flow and branch power.

- (1) Node voltage constraints

The allowed range of voltage deviation in 10 kV DNs is $-7\% \sim +7\%$ [25].

$$\underline{U}_i \leq |U_i(t)| \leq \overline{U}_i \quad i = 1, 2, \dots, N; t \in [0, T] \quad (6)$$

where $U_i(t)$ is the voltage of node i at the moment t ; \underline{U}_i and \overline{U}_i are the upper and lower limits of the node voltage of node i respectively.

(2) Branch current constraints

Current of overhead lines in 10 kV DNs is shown as follow [26]:

$$|I_{ij}(t)| \leq \overline{I}_{ij} \quad i = 1, 2, \dots, N; t \in [0, T] \quad (7)$$

where $I_{ij}(t)$ is the current of branch ij at moment t ; \overline{I}_{ij} is the upper limit of the branch current of branch ij .

(3) Output active/reactive power of PVs constraints

During the whole dispatch period, the output active power of the adjustable PVs cannot exceed its upper limit, the constraint conditions are shown as follows:

$$\begin{cases} |P_i^{\text{PV}}(t)| \leq \overline{P}_i & i \in \Theta; t \in [0, T] \\ |Q_i^{\text{PV}}(t)| \leq \overline{Q}_i & i \in \Theta; t \in [0, T] \end{cases} \quad (8)$$

where Θ is the set of nodes that the PVs access to; $P_i^{\text{PV}}(t)$ and $Q_i^{\text{PV}}(t)$ are output active/reactive powers of the i th PV at the moment t respectively; \overline{P}_i and \overline{Q}_i are the rated output active/reactive powers of the i th PV respectively.

Constraints Equations (6)–(8) can be further modified as follows, which can be solved lineally without absolute value functions.

$$\begin{cases} \underline{U}_i \leq U_i(t) \leq \overline{U}_i & U_i(t) \geq 0 \\ -\overline{U}_i \leq U_i(t) \leq -\underline{U}_i & U_i(t) < 0 \\ I_{ij}(t) \leq \overline{I}_{ij} & I_{ij}(t) \geq 0 \\ I_{ij}(t) \geq -\overline{I}_{ij} & I_{ij}(t) < 0 \\ P_i^{\text{PV}}(t) \leq \overline{P}_i & P_i^{\text{PV}}(t) \geq 0 \\ P_i^{\text{PV}}(t) \geq -\overline{P}_i & P_i^{\text{PV}}(t) < 0 \\ Q_i^{\text{PV}}(t) \leq \overline{Q}_i & Q_i^{\text{PV}}(t) \geq 0 \\ Q_i^{\text{PV}}(t) \geq -\overline{Q}_i & Q_i^{\text{PV}}(t) < 0 \end{cases} \quad (9)$$

(4) Power flow constraints

The active/reactive power of the node that PVs access to must satisfy the constraints shown as follows:

$$\begin{cases} \Delta P_i(t) = P_i^{\text{PV}}(t) - P_i^{\text{load}}(t) - U_i(t) \sum_{j=1}^N U_j(t) (G_{ij} \cos \theta_{ij} + B_{ij} \sin \theta_{ij}) = 0 \\ \Delta Q_i(t) = Q_i^{\text{PV}}(t) - Q_i^{\text{load}}(t) - U_i(t) \sum_{j=1}^N U_j(t) (G_{ij} \sin \theta_{ij} - B_{ij} \cos \theta_{ij}) = 0 \\ P_0(t) \geq 0 \\ Q_0(t) \geq 0 \end{cases} \quad (10)$$

where $P_i^{\text{load}}(t)$ and $Q_i^{\text{load}}(t)$ are the active/reactive load power of the node i at moment t respectively; $U_i(t)$ and $U_j(t)$ are the voltages of node i and node j at moment t respectively; G_{ij} and B_{ij} are the conductance and susceptance of branch ij respectively; θ_{ij} is the voltage phase difference of node i and node j ; $P_0(t)$ and $Q_0(t)$ are the active power and reactive power of the slack node at moment t .

(5) Branch power constraints

The flow power of branch ij needs to meet the constraint conditions shown as follows:

$$\begin{cases} P_{ij}(t) = U_i(t)^2 G_{ij} - U_i(t) U_j(t) (G_{ij} \cos \theta_{ij} + B_{ij} \sin \theta_{ij}) \\ Q_{ij}(t) = U_i(t)^2 B_{ij} - U_i(t) U_j(t) (G_{ij} \sin \theta_{ij} - B_{ij} \cos \theta_{ij}) \end{cases} \quad (11)$$

where $P_{ij}(t)$ and $Q_{ij}(t)$ are the active/reactive power of branch ij at moment t respectively, $i = 1, 2, \dots, N$, $j = 1, 2, \dots, N$.

$$\begin{cases} -\overline{P}_{ij} \leq P_{ij}(t) \leq \overline{P}_{ij} \\ -\overline{Q}_{ij} \leq Q_{ij}(t) \leq \overline{Q}_{ij} \end{cases} \quad (12)$$

where \overline{P}_{ij} and \overline{Q}_{ij} are the upper limits of active/reactive power of branch ij .

(6) ESS charging/discharging constraints

The charging/discharging powers of ESSs, battery capacity and charging/discharging times within a typical day must meet the constraints shown as follows:

$$\begin{cases} -P_{\max} \leq P_{\text{ESS}}^k(t) \leq P_{\max} \\ 20\% \leq \text{SOC}^k(t) \leq 80\% \\ \text{Num}^k \leq 24 \\ \text{SOC}^k(t+1) = \text{SOC}^k(t) + P_{\text{ESS}}^k(t) \end{cases} \quad (13)$$

where P_{\max} is the rated power of ESSs; $P_{\text{ESS}}^k(t)$ is the charging/discharging power of ESS k at moment t ; $\text{SOC}^k(t)$ is the state of charge of the ESS k at moment t ; Num^k is the charging/discharging times of ESSs.

(7) Constraint of dispatch cost of ESSs

Due to the life loss of ESSs in dispatching, the limitation of dispatch cost of ESSs should be satisfied:

$$C_{\text{ESS}} \cdot M \leq \bar{C} \quad (14)$$

where M is the charging/discharging frequency of ESSs in the dispatch period; \bar{C} is the upper level of life loss of ESSs.

The upper and lower limitations of control variables can be designed as the upper level and lower level of individuals in the GA algorithm, such as Constraint Equation (3). The equation constraints of power flows, such as Constraint Equations (4) and (5), are satisfied via the calculation method of forward push back generation power flow. Other inequality constraints are designed as penalty functions in the GA algorithm, such as Constraint Equations (1), (2), (6) and (7). In this paper, we prefer a minimum fitness function in this paper. Hence, when generating each generation of population, whether each individual meets the constraints mentioned in Section 3.2 will be judged first. If any constraint is not satisfied, the value of the fitness function is set as a maximum positive integer, that is, inf.

4 | SOLVING PROCESS BASED ON GENETIC ALGORITHM

In this paper, the ESS security and low-carbon self-adaption day-ahead optimization dispatch strategy in DNs with high proportion PVs is solved by GA. The main reason is that the proposed optimal dispatch model is a nonlinear programming model because of absolute value functions in objectives, which is difficult to be solved directly by the traditional analytic method. Because of the characteristics of self-organisation, self-adaptation and self-learning, GA has a strong advantage in solving complex nonlinear models, and it has been proved that its computing speed and iteration accuracy can meet the requirements [27]. The specific process is as follows:

- 1) The control variables of charging/discharging powers of ESS₁ to ESS_W are converted from decimal continuous variables to M binary numbers with 0-1 variables by coding:

$$B(a) = \left[\begin{array}{c} \underbrace{b_{11}^a \quad b_{12}^a \quad \dots \quad b_{1M}^a}_{\text{ESS}_1 \text{ charging/}} \quad \underbrace{b_{21}^a \quad b_{22}^a \quad \dots \quad b_{2M}^a}_{\text{ESS}_2 \text{ charging/}} \\ \text{discharging power} \quad \text{discharging power} \\ \dots \\ \underbrace{b_{W1}^a \quad b_{W2}^a \quad \dots \quad b_{WM}^a}_{\text{ESS}_W \text{ charging/}} \\ \text{discharging power} \end{array} \right] \quad (15)$$

where a is the individual serial number, $a = 1, 2, \dots, A$, A is the amount of individuals in the population; $B(a)$ is the binary coded string of the a th individual; $b_{n1}^a \quad b_{n2}^a \quad \dots \quad b_{nM}^a$ is the

binary coding string of the n th ESS charging/discharging power in the a th individual.

- 2) The objective functions shown in Formula (3) and (5) are taken as fitness functions under different ESS day-ahead optimization dispatch modes. The fitness functions are modelled as follows.

$$f^1(a) = F_0^{-1}(a) = \begin{cases} 1/F_1 & \text{Mode 1} \\ 1/F_2 & \text{Mode 2} \end{cases} \quad (16)$$

- 3) The selection probability factor P_{sel}^1 can be calculated by the roulette method through Formula (17).

$$P_{\text{sel}}^1 = f^1(a) / \sum_{a=1}^A f^1(a) \quad (17)$$

- 4) The crossover probability factor $P_{\text{cro}} = 0.8$ and the mutation probability factor $P_{\text{var}} = 0.05$ in this paper.
- 5) Get the next generation population based on the selection probability factor, crossover probability factor and mutation probability factor. Then calculate the individual fitness and repeat steps 3) and 4), and determine whether the termination condition of iteration is satisfied; if satisfied, the individual with the largest fitness will be recorded and the calculation will be terminated.
- 6) Determine whether the termination condition of iteration is satisfied; if satisfied, the individual with the largest fitness will be recorded and the calculation will be terminated.
- 7) Decode the binary coding string $B^i(a)$ of the optimal solution into W decimal numbers, which is the optimal solution of the charging/discharging powers of W ESSs.

$$D(n) = R_n + \frac{T_n - R_n}{2^M - 1} \sum_{m=1}^M b_{nm}^{ia} 2^{m-1} \quad (18)$$

where $D(n)$ is the optimal charging/discharging power of the n th ESS, $n = 1, 2, \dots, W$; R_n and T_n is the lower and upper limits of the n th ESS power respectively; b_{nm}^{ia} is the m th binary encoding of the n th ESS in the optimal solution $B^i(a)$.

5 | CASE STUDIES AND RESULTS

5.1 | Case background

Taking into account the practical voltage levels in China, the superiority of the proposed method is verified by a modified 10 kV IEEE 33-node DN shown in Figure 3 [28, 29]. The temporal carbon emission intensity of the slack node is shown in Figure 4a, the access positions of distributed PVs with a rated active power of 200 kW are given in Figure 3, whose temporal output is shown in Figure 4b. The installation locations of distributed ESSs with the rated power and capacity of 200 kW/500 kWh are also given in Figure 3. The total power

demand of loads of the simulated DN is $3.715 + j0.950$ MVA, whose temporal curve of the load power is shown in Figure 4c.

5.2 | Case analysis

In order to verify the proposed ESS security and low-carbon self-adaption optimization dispatch method, the significance of the differences between Case 1 to Case 4 lies in demonstrating the benefits of different dispatch strategies for ESSs in terms of carbon reduction, voltage stability, and overall system performance. The following comparison cases are designed:

Case 1 Without regulation.

Case 2 ESSs participate in low-carbon dispatch according to Mode 2.

Case 3 ESSs participate in voltage regulation mode according to Mode 1.

Case 4 ESSs participate in the dual-mode dispatch adaptively according to the proposed dispatch method containing Mode 1 and Mode 2.

Table 1 shows the security and low-carbon indexes of the simulated DN under different ESS control modes in Case 1 to Case 4. As for the carbon emission reduction capability, carbon

emissions in the whole DN are the smallest when the ESSs participate in the low-carbon dispatch by adopting the Mode 2 in the typical day. The total carbon emission of Case 2 is 4.16×10^7 gCO₂, and the carbon emission reduction of Case 4, Case 1 and Case 3 are ranked by descending order. As for the voltage regulation effect, the total amount of voltage deviation is the smallest when the ESSs participate in voltage control by adopting the Mode 1 during the typical day. The total voltage deviation of Case 3 is 40.67 p.u., and the voltage deviation of Case 4, Case 1 and Case 2 are ranked by an ascending order. Comparing the above four cases, it can be seen that the best low-carbon operation benefit of the DN can be ensured while the ESSs participate in low-carbon dispatch, but the risk of voltage violation in Case 2 is the largest. In Case 3, ESSs participate in voltage control according to Mode 1 can obtain the best effectiveness of the security in the DN, but the carbon emission is the largest. However, the total carbon emission in the dual-mode dispatch scenario is 4.27×10^7 gCO₂ as shown in Case 4, which is only 2.64% higher than that of the best carbon emission reduction effect in Case 2. The total voltage deviation of Case 4 is 41.32 p.u., which is only 1.60% higher than the best voltage regulation effect in Case 3. The dispatch strategy of ESSs in the paper is to achieve less carbon emission under the condition that the voltage does not exceed the limit, although the carbon reduction effect of Case 2 is the best, there is the risk of voltage violation. According to Table 1, under the premise of ensuring the secure operation of the DN, the voltage deviation of Case 4 increases by 1.60% compared with Case 3, but the carbon emission decreases by 4.00×10^5 gCO₂. In summary, on the basis of controlling the risk of voltage violation, the carbon emission reduction is maximised by the ESS self-adaption dispatch method proposed in this paper.

From the perspective of carbon emission reduction, the carbon emissions of the whole DN shown in Figure 5 have significant temporal characteristics. Since Case 1 does not involve ESS dispatch, we use the temporal carbon emissions in Case 1 as a baseline to analyse the differences in the remaining

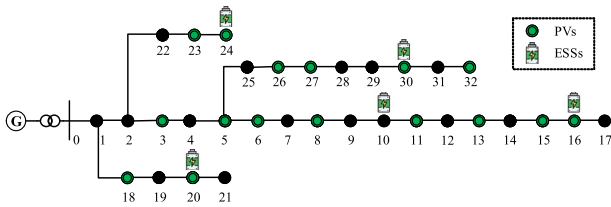


FIGURE 3 The modified 10 kV IEEE 33-node distribution network.

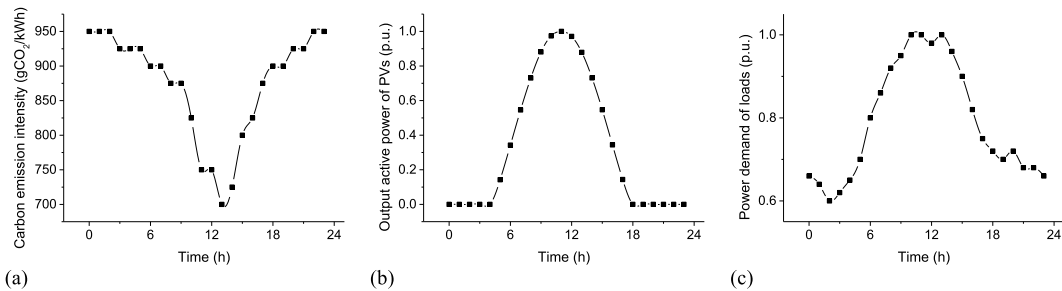


FIGURE 4 Temporal curve of nodal carbon emission intensity of the slack node, output power of proportion of photovoltaics and power demand of loads (a) Nodal carbon emission intensity of the slack node; (b) Output power of PVs; (c) Power demand of loads.

	Case 1	Case 2	Case 3	Case 4
Total carbon emissions in 24 h (gCO ₂)	4.47×10^7	4.16×10^7	4.31×10^7	4.27×10^7
Total node voltage deviation in 24 h (p.u.)	42.18	41.92	40.67	41.32

TABLE 1 Indexes of carbon emissions and voltage deviation of Case 1- Case 4 in the modified 10 kV IEEE 33-node distribution network.

three dispatch modes. From 12:00–13:00, the carbon emission of Case 1 is the lowest at 0.63 t . During this period, in the low-carbon operation mode (Case 2), the carbon emission is 0.22 t , resulting in a reduction of 64.63% compared to Case 1. In the dual-mode operation (Case 4), the carbon emission is 0.42 t , which corresponds to a reduction of 34.18% compared to Case 1. However, in the voltage regulation mode (Case 3), the carbon emission is 1.33 t , representing an increase of 1.1 times compared to Case 1. From 20:00–21:00, the carbon emission of Case 1 is the highest at 2.69 t . In the dual-mode operation (Case 4), the carbon emission is 1.79 t , resulting in a reduction of 33.38% compared to Case 1. However, in the low-carbon operation mode (Case 2), the carbon emission is 3.48 t , representing an increase of 29.27% compared to Case 1. In the voltage regulation mode (Case 3), the carbon emission is 3.56 t , which is 32.58% higher than that of Case 1. During the peak period of PVs outputs, a high proportion of distributed PVs can adequately provide powers all loads in the DN, while the carbon emissions of the whole DN can be reduced significantly. When the peak value of load demands and the valley value of PVs' output powers occur simultaneously, Case 2 to Case 4 lead to a decrease of carbon emissions due to the advantage of ESSs transferring low-carbon electricity, where Case 2 shows the lowest carbon emission. The carbon emission reduction of Case 4 is similar to Case 2 once no risk of voltage violation occurs in the DN, otherwise, the operation mode will be switched to Mode 1 to reduce the voltage fluctuation of the whole DN.

In addition, the carbon emission intensity of the slack node is affected by the proportion of power generations with different carbon emission intensities in the upper-level power grid. The main reason is that the temporal characteristics of low-carbon sources, such as large-scale PVs, have a strong correlation with the output characteristics of distributed generations in the DN. Therefore, the temporal fluctuation characteristics of the carbon emission intensity of the slack node will exacerbate the peak-valley difference rate of the carbon emission intensity of the DN, more frequent charging/discharging of ESSs are resulted, and the depth of charging/discharging is increased.

From the perspective of voltage regulation, the voltage deviation of each node is also affected by the temporal characteristics of distributed PVs output as shown in Figure 6. In Case 1, no ESS participates in voltage regulation, the voltages

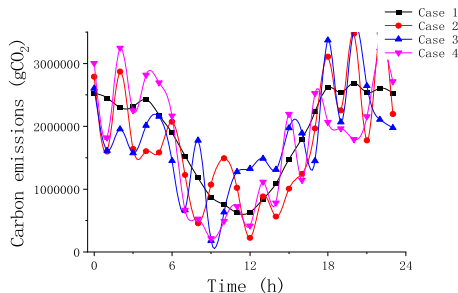


FIGURE 5 Temporal curves of carbon emissions in Case 1-4.

of nodes near the access positions of PVs exceed the upper limit with a peak output power of PVs, and the nodes at the end of the feeder suffer from undervoltage with a valley output power of PVs. In Case 2, the ESS dispatch strategy with the goal of carbon emission reduction can partly alleviate the problem of undervoltage, but the overvoltage cannot be settled significantly. In Case 3, the dispatch strategy of ESSs is carried out with the goal of voltage regulation, and voltages of all nodes in the DN are limited within the allowable range of 0.93 p.u.–1.07 p.u. during the dispatch period, and the voltage deviation of the whole DN can be guaranteed to the smallest level. On the basis of Case 2, Case 4 further considers the node voltage constraints of the switch principle in the security and low-carbon operation mode, more frequent switches are certainly caused as shown in Figure 8c. Besides, the carbon emission reduction is also maximised on the basis of controlling the risk of voltage violation in the whole DN.

In Case 1, there is no dispatch of ESSs. In Case 2, the ESSs operate in Mode 2 continuously, aiming to minimise the overall carbon emissions. In Case 3, the ESSs operate in Mode 1 continuously, with the objective of ensuring voltage safety. The temporal dual-mode switching of ESSs in Case 4 is illustrated in Figure 7. The ESSs operate in Mode 2 from 6:00–9:00, during which the voltage deviations are relatively small due to lower load demands, allowing for low-carbon operation. Additionally, the ESSs operate in Mode 2 from 14:00–17:00, corresponding to a high peak of PVs output and relatively

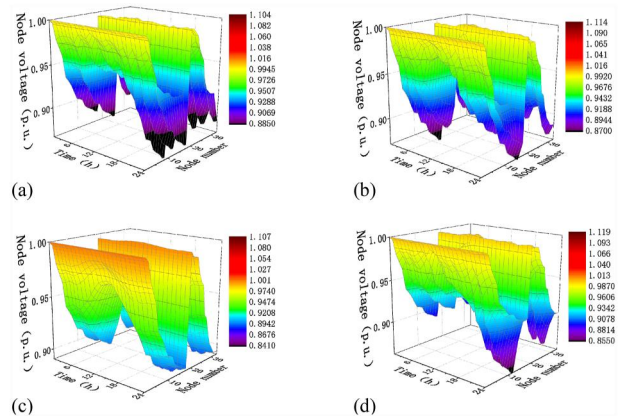


FIGURE 6 Temporal curves of voltage deviation of each node in Case 1-Case 4 (a) Case 1; (b) Case 2; (c) Case 3; (d) Case 4.

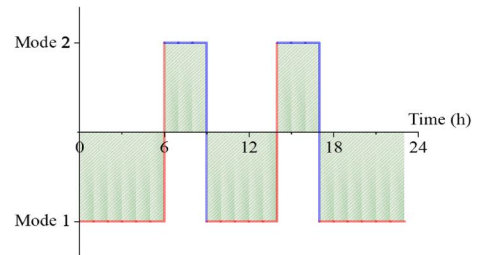


FIGURE 7 Temporal dual-mode switching of energy storage systems in Case 4.

moderate load demands, enabling low-carbon operation. For the remaining dispatch periods, the ESSs operate in Mode 1 to ensure voltage safety across the entire DN.

To further analyse the charging/discharging characteristics of ESSs under different control modes, the temporal charging/discharging powers of ESSs are gained as shown in Figure 8. Note that this paper defines the charging powers of ESSs as positive and the discharging powers as negative. The switch times of ESSs at the middle of the feeder is less compared with those at the end of the long feeder, and the depth of charging/discharging of ESSs at the middle of the feeder is lower, too. The main reason is that the access positions of distributed PVs is near to the end of the feeder, where the risk of node voltage violation is higher. The red and purple ellipses in the Figure 8 enclose the peak and valley periods of the PV output, respectively. It can be roughly observed that in Case 4, compared to Case 2 and Case 3, there is a higher charging of ESSs during the high PV output periods, while there is a higher discharging of ESSs during the low PV output periods. Then, the charging/discharging powers of ESSs under different control modes of Case 2 and Case 4 are compared and analysed. In Case 2, to reduce the carbon emissions of the whole DN, the charging/discharging frequency of ESSs is high and the charging/discharging powers are large by realizing the flexible temporal transfer of low-carbon electricity. In Case 3, in order to eliminate the risk of voltage violation and reduce the voltage deviation, the charging/discharging frequency of ESSs is low and the charging/discharging powers are relatively

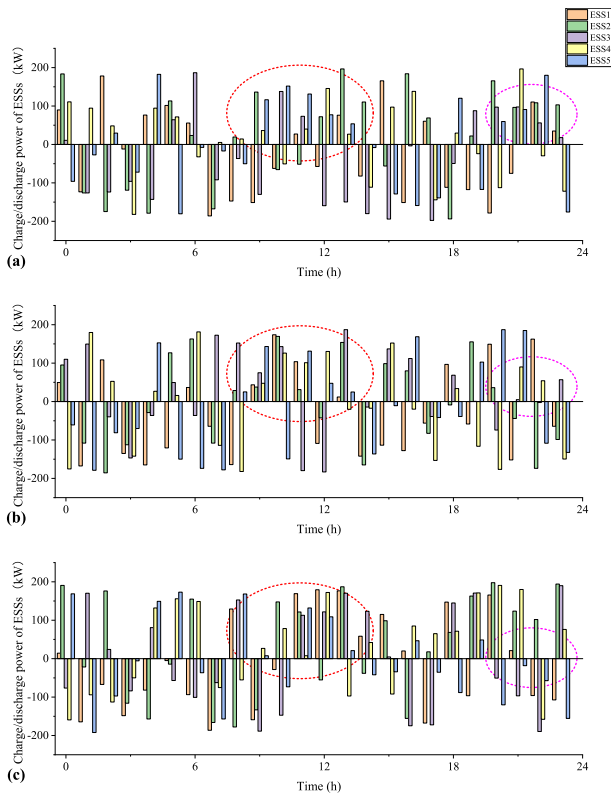


FIGURE 8 Temporal charging/discharging powers of energy storage systems in Case 2–Case 4. (a) Case 2; (b) Case 3; (c) Case 4.

small. In Case 4, the charging/discharging frequency and powers of ESSs are at the compromise level of Case 2 and Case 3, the charging/discharging frequency and depth of ESSs can be adaptively adjusted through flexible switches of operation modes, and then the security and low-carbon operation can be realized by controlling the risk of voltage violation and improving the carbon emission reduction effect of the DN.

Moreover, this paper also analyses the differences between low-carbon operation and traditional economic operation mode of ESS charging/discharging dispatch strategies. As shown in Figure 9, the main regulation goal under economic operation is to reduce the power loss in the dispatch period, and ESSs mainly play the role of peak-load shedding and shifting. During peak load periods such as 11:00–12:00 and 18:00–20:00, ESSs provides the power required by the load through discharge to reduce the amount of electricity purchased from the superior power grid and thus reduce the power loss of the whole DN. In addition, since the internal remaining electricity of ESSs is generated by clean energy, its carbon emission is 0, which can also achieve the effect of carbon reduction. During the load trough and peak hours of photovoltaic power generation, such as 13:00–16:00, ESSs realize the consumption of new energy through charging, thus reducing the power loss of the whole network. However, under the low-carbon operation mode, the operation and dispatch of ESSs are only aimed at improving the utilization rate of new energy, without considering the impact of the charging/discharging action on the power loss. The charging/discharging strategy is different from the traditional economic operation mode to some extent.

Further analysis of low-carbon operation and the traditional mode of economic operation of carbon emissions and the power loss, ESSs in Case 2 only participate in low-carbon dispatching minimum cut carbon emissions, is 41.6 t, economic operation scenarios carbon emissions increased by 13.51%. In the economic operation scenario, the power loss of the whole network is the minimum, which is 137.83 kWh, which is 22.01% less than that of the low-carbon operation mode in Case 2% and 22.96% less than that of the dual operation modes in Case 4.

Further considering the reactive power regulation capacity of photovoltaic inverters, the reactive power regulation of photovoltaic inverters installed at node 15 and 16 can reduce the total voltage offset of the whole network to 38.90 p. u. and

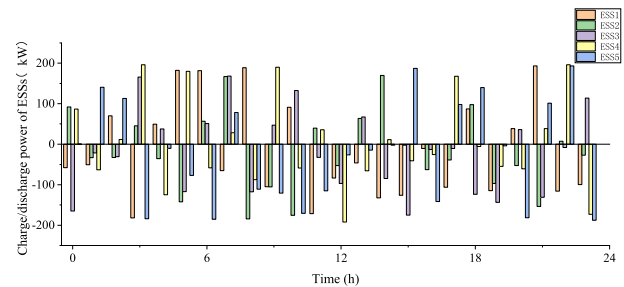


FIGURE 9 Temporal charging/discharging power of energy storage systems under economic operation.

the total carbon emission to 40.80 t. The temporal charging/discharging power of ESSs under this dispatch strategy is shown in Figure 10. It can be seen that adding consideration to the reactive power regulation capacity of PV inverters on the basis of ESS regulation can improve the voltage deviation and carbon reduction effect of the whole network to a certain extent, and obtain different dispatch strategies. However, it is still applicable to the generation of the safety-low carbon adaptive dispatch architecture proposed in this paper, which proves the applicability and scalability of the adaptive optimal dispatch strategy proposed in this paper.

5.3 | Large-scale case study

In order to verify the proposed ESS security and low-carbon self-adaption optimization dispatch method in medium/large-scale DNs, this case study is conducted on the modified 10 kV IEEE 123-node DN, which has been converted into a three-phase balanced network. The topology structure is presented in the form of a single-line diagram. The network is equipped with 50 sets of PVs and 10 sets of ESSs. The installation locations of the PVs and ESSs are depicted in Figure 11. Each PV unit has a capacity of 50 kWh, while each ESS unit has a capacity of 50 kWh and a rated power

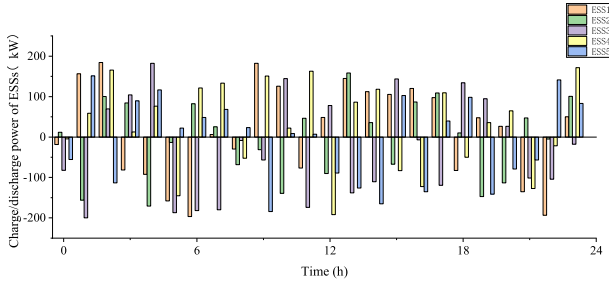


FIGURE 10 Temporal charging/discharging power of energy storage systems considering the reactive power regulation capacity of proportion of photovoltaic inverters.

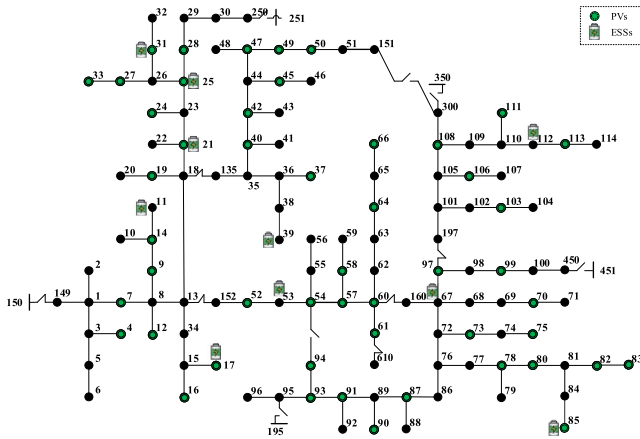


FIGURE 11 The modified 10 kV IEEE 123-node distribution network.

of 20 kW. The comparison cases are designed to be consistent with those in the modified 10 kV IEEE 33-node DN.

In this case study, based on the same comparative classification method as mentioned in the modified 10 kV IEEE 33-node DN, four sets of cases, namely Case 1 to Case 4, are established. The results in Table 2 indicate that Case 2, which dispatches the ESSs in the low-carbon operation mode, achieves the lowest overall carbon emissions, followed by Case 4. Case 3, which employs the voltage regulation mode for the ESSs dispatch, exhibits the smallest voltage deviations among all nodes over a 24-h period, with Case 4 coming next. On the other hand, Case 1, where the ESSs are not involved in the dispatch, shows the highest values for both carbon emissions and voltage deviations. In summary, Case 4 minimises carbon emissions to the maximum extent while ensuring voltage safety. This is consistent with the results in the modified 10 kV IEEE 33-node DN, thereby validating the applicability and effectiveness of the proposed method in medium/large-scale DNs.

6 | CONCLUSION

In this paper, the proposed two-stage self-adaption security and low-carbon dispatch strategy of ESSs in DNs with high proportion PVs shows significant advantages in controlling the risk of voltage violation and improving carbon emission reduction.

- (1) Based on the flexible switch between low-carbon dispatch mode and voltage regulation mode, the proposed security and low-carbon self-adaption dispatch method of ESSs can greatly decrease the carbon emission and the risk of voltage violation caused by the high proportion PVs in DNs. Verified by the case studies, the carbon emission of the simulated DN can be reduced by 4.68% due to the characteristics of ESSs temporally transferring the low-carbon electricity.
- (2) The two-stage dispatch strategy of the ESS can effectively address the randomness and volatility of low-carbon power sources such as PVs by taking into account the temporal characteristics of carbon emission intensity of the upper power grid. It is also applicable to scenarios that consider the voltage regulation ability of reactive powers of PV inverters, enabling dual-mode adaptive collaborative

TABLE 2 Indexes of carbon emissions and voltage deviation of Case 1-Case 4 in the modified 10 kV IEEE 123-node distribution network.

	Case 1	Case 2	Case 3	Case 4
Total carbon emissions in 24 h (gCO_2)	4.18×10^7	4.06×10^7	4.13×10^7	4.12×10^7
Total node voltage deviation in 24 h (p.u.)	346.89	345.03	339.68	343.02

regulation between PVs and ESSs. This leads to an improved carbon reduction effect for the entire DN and reduced voltage fluctuation.

As an outlook, with the increasing flexibility of active DNs, multiple resources and loads can participate in carbon reduction in the entire energy system. Based on the proposed dual-mode dispatch framework, more potential measures can be taken into consideration by accurately depicting their carbon reduction capabilities and dispatching them properly.

AUTHOR CONTRIBUTION

Lei Chen: Methodology; Software; Validation; Formal analysis; Writing - Original draft; Visualization. **Wei Tang:** Conceptualization; Writing - Review & Editing; Project Administration. **Lu Zhang:** Supervision; Writing - Review & Editing; Funding acquisition. **Zhaoqi Wang:** Writing - Review & Editing. **Jun Liang:** Supervision; Writing - Review & Editing.

ACKNOWLEDGEMENTS

This work was supported by Science and Technology Project of State Grid Corporation of China “Research and Development of Key Technologies for Economic and Low-Carbon Regulation of New-Type Rural Power Grids with Massive Distributed Resources” (1400-202155508A-0-5-ZN).

CONFLICT OF INTEREST STATEMENT

The authors declare that they have no known competing financial interests or personal relationships that could have appeared to influence the work reported in this paper.

DATA AVAILABILITY STATEMENT

The data that support the findings of this study are available from the corresponding author upon reasonable request.

ORCID

Lei Chen  <https://orcid.org/0000-0002-0921-4107>

Lu Zhang  <https://orcid.org/0000-0001-5696-2418>

Zhaoqi Wang  <https://orcid.org/0000-0002-4035-2612>

REFERENCES

- Zhang, S., Chen, W.: Assessing the energy transition in China towards carbon neutrality with a probabilistic framework. *J. Nat Commun.* 13(1), 87 (2022). <https://doi.org/10.1038/s41467-021-27671-0>
- Wang, F., et al.: Technologies and perspectives for achieving carbon neutrality. *J. The Innovation.* 2(4), 100180 (2021). <https://doi.org/10.1016/j.xinn.2021.100180>
- Kang, C., et al.: Key scientific problems and research framework for carbon perspective research of new power systems. *J. Power System Technology* 46(03), 821–833 (2022). <https://doi.org/10.13335/j.1000-3673.pst.2021.2550>
- Alizadeh, A., et al.: Energy management in microgrids using transactive energy control concept under high penetration of Renewables; A survey and case study. *Renew. Sust. Energ. Rev.* 176, 113161 (2023). <https://doi.org/10.1016/j.rser.2023.113161>
- Zhang, L., et al.: Intra-day correction strategy of plan for AC/DC hybrid distribution network based on spatio-temporal power coordination. *J. Automation of Electric Power Systems.* 45(24), 106–114 (2021). <https://doi.org/10.7500/AEPS20210608001>
- Wang, Y., et al.: Research on economic scheduling of ES peak and frequency regulation based on dynamic peak-valley time division. *J. Electric Power.* 55(08), 64–72 (2022)
- Nan, B., et al.: Optimal configuration of energy storage in PV-storage microgrid considering demand response and uncertainties in source and load. *J/OL. Power System Technology*, 1–12 (2022). <https://doi.org/10.13335/j.1000-3673.pst.2022.0798>
- Chai, Y., et al.: Network partition and voltage coordination control for distribution networks with high penetration of distributed PV units. *J. IEEE T Power Syst.* 33(3), 3396–3407 (2018)
- Tang, W., et al.: Coordinated control of photovoltaic and energy storage system in low-voltage distribution networks based on three-phase four-wire optimal power flow. *J. Automation of Electric Power Systems* 44(12), 31–40 (2020). <https://doi.org/10.7500/AEPS20190609004>
- Wong, J., Lim, Y.S., Morris, E.: Novel fuzzy controlled energy storage for low-voltage distribution networks with photovoltaic systems under highly cloudy conditions. *J. Energ. Eng.* 141(1), B4014001 (2015). [https://doi.org/10.1061/\(ASCE\)EY.1943-7897.0000178](https://doi.org/10.1061/(ASCE)EY.1943-7897.0000178)
- Wang, Y., et al.: A voltage regulation method using distributed energy storage systems in LV distribution networks. In: *IEEE International Energy Conference*, pp. 1–6. IEEE, Leuven, Belgium (2016)
- Worthmann, K., et al.: Distributed and decentralized control of residential energy systems incorporating battery storage. *J. IEEE Trans Smart Grid.* 6(4), 1914–1923 (2015). <https://doi.org/10.1109/TSG.2015.2392081>
- Liu, J., et al.: Research on optimization algorithm of active microgrid energy management considering generalized energy storage. *J/OL. Power System Technology.*, 1–11 (2021). <https://doi.org/10.13335/j.1000-3673.pst.2021.1926>
- Li, X., et al.: Optimal allocation of energy storage in renewable energy grid considering the demand of peak and frequency regulation. *J/OL. Energy Storage Science and Technology*, 1–11 (2022). <https://doi.org/10.19799/j.cnki.2095-4239.2022.0331>
- Wang, X., et al.: Optimal allocation of a wind-PV-battery hybrid system in smart microgrid based on particle swarm optimization algorithm. *J. Integrated Intelligent Energy.* 44(06), 52–58 (2022). <https://doi.org/10.3969/j.issn.2097-0706.2022.06.006>
- Shabani, M., et al.: Techno-economic comparison of optimal design of renewable-battery storage and renewable micro pumped hydro storage power supply systems: a case study in Sweden. *J. Appl Energy.* 279, 115830 (2020). <https://doi.org/10.1016/j.apenergy.2020.115830>
- Campana, P.E., et al.: Li-ion batteries for peak shaving, price arbitrage, and photovoltaic self-consumption in commercial buildings: a Monte Carlo analysis. *J. Energy Conversion Manage.* 234, 113889 (2021). <https://doi.org/10.1016/j.enconman.2021.113889>
- Ren, H., et al.: Optimal deployment of distributed rooftop photovoltaic systems and batteries for achieving net-zero energy of electric bus transportation in high-density cities. *J. Appl Energy.* 319, 119274 (2022). <https://doi.org/10.1016/j.apenergy.2022.119274>
- Zhang, L., et al.: Optimal configuration strategy of mobile energy storage in distribution network considering balance between resilience and economy. *J. Automation of Electric Power Systems.* 44(21), 23–31 (2020). <https://doi.org/10.7500/AEPS20200222006>
- Kang, C., et al.: Carbon emission flow from generation to demand: a network-based model. *J. IEEE Trans Smart Grid.* 6(5), 2386–2394 (2015). <https://doi.org/10.1109/TSG.2015.2388695>
- Sun, Y., et al.: Day-ahead optimization schedule for gas-electric integrated energy system based on second-order cone programming. *CSEE J. Power Energy Syst* 6(1), 142–151 (2020). <https://doi.org/10.17775/CSEEJPES.2019.00860>
- Chen, H., et al.: Collaborative optimal operation of transmission system with integrated active distribution system and district heating system based on semi-definite programming relaxation method. *Energy* 227, 120465 (2021). <https://doi.org/10.1016/j.energy.2021.120465>
- Khalil, G., et al.: Accuracy enhancement of second-order cone relaxation for AC optimal power flow via linear mapping. *Elec. Power Syst. Res.* 212, 108646 (2022). <https://doi.org/10.1016/j.epsr.2022.108646>

24. Sayed, A.R., et al.: Distribution-level robust energy management of power systems considering bidirectional interactions with gas systems. *IEEE Trans. Smart Grid* 11(3), 2092–2105 (2020). <https://doi.org/10.1109/TSG.2019.2947219>
25. Power quality allowable deviation of supply voltage. GB/T 12325-2008. (2008)
26. Round wire concentric lay overhead electrical stranded conductors. GB/T 1179-2008. (2008)
27. Alkaran, S.D., et al.: Optimal overcurrent relay coordination in interconnected networks by using fuzzy-based GA method. *J. IEEE Trans. Smart Grid*. 9(4), 3091–3101 (2018). <https://doi.org/10.1109/TSG.2016.2626393>
28. Wang, Z., et al.: Equilibrium allocation strategy of multiple ESSs considering the economics and restoration capability in DNs. *Appl. Energy* 306, 118019 (2022). <https://doi.org/10.1016/j.apenergy.2021.118019>
29. Zhang, L., et al.: A coordinated restoration method of hybrid AC–DC distribution network with electric buses considering transportation system influence. *IEEE Trans. Ind. Inf.* 18(11), 8236–8246 (2022). <https://doi.org/10.1109/TII.2022.3161027>

How to cite this article: Chen, L., et al.: Two-stage self-adaption security and low-carbon dispatch strategy of energy storage systems in distribution networks with high proportion of photovoltaics. *IET Smart Grid*. 1–13 (2023). <https://doi.org/10.1049/stg2.12118>